Chemical Methodologies 6(2022) 661-676

Chemical Methodologies

Journal homepage: http://chemmethod.com

*Original Research Article*

# Adsorption and Photocatalytic Degradation of Crystal Violet Dye under Sunlight Irradiation Using Natural and Modified Clays by Zinc Oxide

**Zakarya Ayoub Messaoudi[1,*], Driss Lahcene[2], Tahar Benaissa[1], Mohammed Messaoudi[3], Brahim Zahraoui[2], Meriem Belhachemi[2], Abderrahim Choukchou-Braham[4]**

[1]*Laboratory of Physicochemical Studies, University of Saida - Dr. Moulay Tahar, Algeria*
[2]*Laboratory of Chemistry and Environmental Science, Faculty of Exact Sciences, University of TAHRI Mohamed Bechar, BP 417 Kenadsa Road, Bechar 08000, Algeria*
[3]*Department of Life and Natural Sciences, University of Adrar - Ahmed Draia, Algeria*
[4]*Laboratory of Catalysis and Synthesis in Organic Chemistry, University of Tlemcen, B.P. 119 Tlemcen 13000, Algeria*

**ARTICLE INFO**

**Article history**

Submitted: 2022-04-02
Revised: 2022-05-26
Accepted: 2022-06-26
Manuscript ID: CHEMM-2205-1507
Checked for Plagiarism: **Yes**
Language Editor:
Dr. Behrouz Jamalvandi
Editor who approved publication:
Professor Dr. Ali Ramazani

**DOI**:10.22034/CHEMM.2022.340376.1507

**KEYWORDS**

Clay
ZnO
Crystal violet dye
Impregnation
Adsorption; Photocatalysis
Sunlight irradiation

**ABSTRACT**

A ZnO-supported natural volcanic Algerian clay (ZnO/CNA) was synthesized through an impregnation method to prepare a photocatalytic adsorbent integrated. The discoloration of crystal violet dye (CV) from an aqueous solution was carried out using natural and modified clays via zinc oxide by adsorption and photocatalytic degradation. The materials were characterized through X-ray fluorescence spectrometer (XRF), Scanning electronic microscopy (SEM), Energy-dispersive X-ray spectroscopy (EDX), Fourier transform infrared spectroscopy (FTIR), and X-ray diffraction (XRD). The effects of diverse experimental parameters on the adsorption process efficiency were investigated. The photocatalysis process of CV was executed by the ZnO/CNA material under sunlight irradiation. The characterization results informed that ZnO nanoparticles were well dispersed on the clay surface (CNA). The adsorption experiments were well clarified via the kinetic model of pseudo-second-order and isotherm model of Langmuir with correlation coefficients (R2 > 0.99). Moreover, thermodynamic data showed that CV adsorption was endothermic, spontaneous, and physical. The adsorption capacity of CV was high utilizing ZnO/CNA material and gives 74.63 mg/g by the Langmuir equation. The photodegradation kinetics followed pseudo-1st order approximate the model of Langmuir-Hinshelwood. The discoloration efficiency with the ZnO/CNA (~ 92%) was higher compared with the CNA (67%), clearly suggesting promoting effect of ZnO.

**GRAPHICAL ABSTRACT**


* Corresponding author: Zakarya Ayoub Messaoudi
✉ E-mail: zakarya.messaoudi@univ-saida.dz

## Introduction

The dyeing effluents are one of the worldwide principal problems of water pollution that affects human health and the environment, found in several industries such as textiles, ceramics, plastics, papers, cosmetics, medicines, etc. [1, 2]. Dyes are discharged into wastewater and cause serious environmental problems. Among these dyes, crystal violet is a synthetic and cationic triphenylmethane dye that is employed broadly as a textile dye and has various applications in industrial and medical domains [3, 4]. Crystal violet dye has effects on human health among them, a strong carcinogen, and causes genetic mutations [5]. The elimination of toxic dyes from wastewater is an important issue facing the textile dyeing industry. Clay materials are widely used in wastewater treatment and are among the cheapest, most abundant, ion exchangeable, environmentally friendly, and non-toxic materials [6, 7]. For this reason, clay has been studied and developed as an extremely efficient adsorbent for various applications and functions for the removal of dye from wastewater [8, 9]. Several physicochemical methods were researched to eliminate toxic dyes; the adsorption process is considered the simplest and most efficient method with easy operational conditions [10, 11]. Among the promising technologies used for wastewater treatment is photocatalysis, which is considered an efficient, performing process and environmentally friendly [9]. Heterogeneous photocatalytic degradation is used widely to remove toxic dyes from wastewater by solid materials and light sources; in this regard, there are recent works reported by many developers [12, 13], but a few studies have used ZnO-supported natural clay in photodegradation of CV dye from aqueous solution under sunlight irradiation. To enhance the clay material, we added zinc oxide as an active phase which has a positive and promoter effect on the adsorption and photodegradation activity [14]. In this work, natural Algerian clay (CNA) was acting as a support for ZnO nanoparticles via the impregnation method [15]. The materials were characterized by different techniques and analyses. The ZnO/CNA material is considered an efficient adsorbent and photocatalyst in the discoloration of CV solution. The influence of main experimental parameters on the process of adsorption were investigated, including initial dye concentration, initial pH solution, temperature, and contact time along with the isotherms, kinetics, and thermodynamics. In addition, the photodegradation activity of ZnO/CNA material was assayed under direct irradiation sunlight.

## Materials and Methods

Crystal violet dye (CV, cationic, chemical formula $C_{25}H_{30}ClN_3$, M = 407.98 g/mol) used in this work was purchased from Honeywell Fluka. Zinc acetate dihydrate ($ZnC_4H_6O_4.2H_2O$, M = 219.5 g/mol, ≥ 98%) was supplied by Sigma-Aldrich chemical and used as a ZnO source for the synthesized of ZnO/CNA material. The natural clay (CNA) was sourced locally in southern Algeria from the area of Aïn Ouarka [16]. The raw clay was first purified from impurities and coarse particles by the sedimentation method for obtaining a smaller size particle than 2 µm. The purified clay was dried at 60 °C and then calcined for 4 hours at 500 °C under static air with a constant rate equal to 2 °C/min. The ZnO/CNA material was synthesized via an impregnation method with a ZnO/CNA weight ratio of 15:85. First, 5.1 g of CNA was put in a vessel and heated at 60 °C using a sand bath. Under stirring, the CNA was impregnated with a precursor solution that contained dehydrated zinc acetate (2.43 g) dissolved in 40 mL of distilled water. Then, the mixture was left overnight in the oven at 120 °C. Finally, the ZnO/CNA material was calcined with the same conditions as above (500 °C, 4 h, 2 °C/min). The required quantity of CV was dissolved in distilled water for the preparation of the stock solution (1 g/L). The stock solution was diluted for obtaining the intended concentration for the adsorption and photocatalytic degradation experiments.

### *Clays and photocatalysts characterization*

Numerous techniques of analysis were used for characterized the materials. X-ray fluorescence spectrometer (Philips analytical) analysis determined the chemical composition of natural clay. The identification of the different phases was studied by an X-ray diffractometer (Proto AXRD Benchtop), with CuKα (λ =1.5418 Å) radiation in the range 2θ of 10°-90° at a scanning rate of 0.02°/s. The investigation of the morphology and

the structure of the CNA and ZnO/CNA material was carried out by scanning electron microscopy (JEOL JSM-7610FPlus). The chemical composition present in the ZnO/CNA catalyst was evaluated by energy dispersive X-ray spectrometry (EDX - Bruker XFlash® 6-30 detector). FTIR spectra were obtained by Fourier transform infrared spectrometer (Agilent Cary 660 FTIR, KBr Pellet), with a wavelength ranging from 4000-400 $cm^{-1}$ to study the surface functional groups.

*Adsorption experiments*

In these experiments, the CV adsorption over CNA or ZnO/CNA materials was realized in 100 mL Erlenmeyer flasks holding 50 mL of aqueous dye solution, 0.025 g of materials, and pH of 6.7 with an initial concentration of CV dye by 25 mg/L at ambient temperature. The reaction mixture was magnetically stirred for 400 rpm. After, 2 mL was withdrawn from the suspension for each sample at particular time intervals and then centrifuged for 10 min at 4000 rpm to remove the remaining material particles in the solution. The CV concentration was analyzed through a UV-vis spectrophotometer at $\lambda_{max}$ of crystal violet dye (583 nm). Percentage removal efficiency and the adsorbed quantity of dye to adsorbent unit mass (mg/g) at equilibrium were determined by these equations [17]:

$$\text{Removal efficiency (\%)}=\frac{C_0-C_t}{C_0}\times 100 \quad (1)$$

$$\text{Adsorption capacity } q_e=(C_0-C_e)\times\frac{V}{m} \quad (2)$$

where $C_0$ (mg/L), $C_e$ (mg/L), and $C_t$ (mg/L) are the concentrations of dye initially at (t = 0), equilibrium, and at time t, respectively, m is the mass of materials (g) and V is the volume of solution (L).

The effect of the main experimental parameters on the adsorption efficiency was investigated as follows: the contact time (0-180 min), CV dye initial concentrations (05 - 200 mg/L), pH of the initial solution (2.0 - 11.0) were adjusted using a 0.1 M solution (HCl or NaOH) to the intended pH value, and thermodynamic studies were estimated at temperatures (313-333 K).

*Adsorption/photodegradation experiments*

The adsorptive/photocatalytic activity of CNA and ZnO/CNA materials were studied in the discoloration of the CV dye solution. The adsorption process study was executed in the dark, while photodegradation was realized under direct sunlight [11, 13]. In each experiment, 0.025 g of material was added to 50 mL of CV dye solution (50 mg/L, pH = 6.7) at ambient temperature. Before irradiation, the resulting suspension was stirred magnetically for 1 hour (in the dark), to reach the equilibrium of the adsorption-desorption between the surface of materials and CV molecules. The adsorption capacities of CNA or ZnO/CNA materials into CV were determined in dark at ambient temperature; the same reaction mixture was then photo-irradiated by sunlight for 2 hours under continuous stirring, where the solar energy was in the order of 200 W. We measured the power of solar energy by fluxmeter. The total adsorption and photocatalytic degradation time followed was 3 hours. Aliquots of 2 mL were withdrawn from the reaction mixture at particular time intervals after periods of adsorption and irradiation, which were centrifuged (4000 rpm, 10 min), and then analyzed to determine CV concentration [18].

## Results and discussion

*Physicochemical characterization*

*X-Ray Fluorescence Spectrometry*

The relative quantity of the principal minerals for the natural clay is presented in Table 1. The elements clinochlore, sericite, and quartz represent the majority of the principal components in the natural clay in proportions estimated a 50%, 45%, and 5%, respectively, which appear in the XRD results. The chemical elements of sericite and clinochlore were measured in (wt %) as sericite: $Al_2O_3$ 32.39, $SiO_2$ 47.36, $K_2O$ 10.05, $Na_2O$ 0.52, CaO 0.19, $TiO_2$ 0.35, MgO 1.59, and FeO 2.28 [19] and clinochlore as: $Al_2O_3$ 18.10, $SiO_2$ 31.13, FeO 3.10, MgO 33.41, $Cr_2O_3$ 0.70, $TiO_2$ 0.06, F 0.29, $Fe_2O_3$ 0.64 [20]. According to these references, the mineralogical rate of the natural clay studied is based on the diversity of two components sericite and clinochlore.

**Table 1**: Chemical compositions of the natural clay

| The samples | Natural clay (%) |
|---|---|
| $SiO_2$ | 37.42 |
| $Al_2O_3$ | 18.72 |
| MgO | 15.69 |
| $Fe_2O_3$ | 6.08 |
| CaO | 5.14 |
| $K_2O$ | 2.68 |
| $Na_2O$ | 1.25 |
| $SO_3$ | 1.17 |
| $TiO_2$ | 0.77 |
| $P_2O_5$ | 0.12 |
| Fire loss | 10.95 |

*Fourier transform infrared spectroscopy*

The spectra of FT-IR obtained for CNA and ZnO/CNA materials are presented in Figure 1. The wideband was observed between 3200 and 3700 $cm^{-1}$ due to the stretching vibration of the group -OH in the clay, or to two Al atoms 3424 $cm^{-1}$ or the atom of Al and an Mg atom 3568 $cm^{-1}$. The band around 2350 $cm^{-1}$ represents the molecules of water in the interlayer which corresponds to the vibrations of deformation. The band at 3430 $cm^{-1}$ of stretching vibration is appointed to the attendance of the groups -OH of water molecules inside the solid material layers [14, 21]. The band of 1630 $cm^{-1}$ is assigned to water bending vibrations. The bands appearing at 768 and 465 $cm^{-1}$ can be attributed to stretching vibrations for Si-O-Al and Si-O-Mg, respectively. The broadband in the range (900 - 1100 $cm^{-1}$) is related to the elongation of the Al-O and/or Si-O bonds. The band of 678 $cm^{-1}$ is characteristic of the deformation vibrations of -OH groups in trioctahedral clay minerals [22, 23].

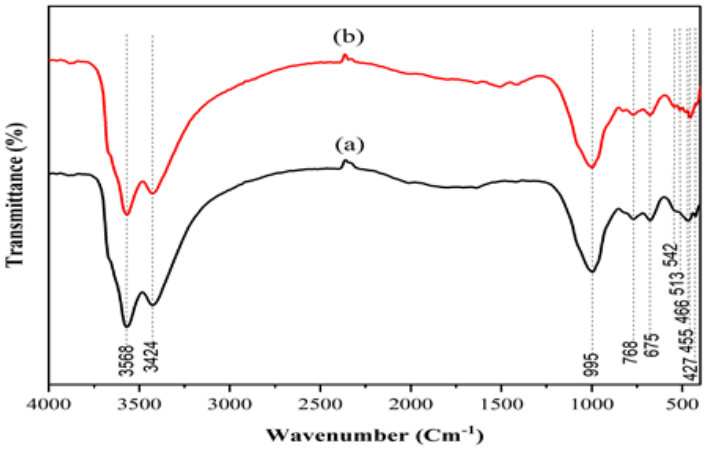


**Figure 1:** FT-IR spectra of a) CNA and b) ZnO/CAN

*X-Ray diffraction analysis*

The diffractogram patterns of CNA and ZnO/CNA materials are illustrated in Figure 2. Each material consists of two mineral phases, which represent clinochlore and sericite 2M1. The clinochlore or called chlorite is a structure minerals type (T-O-T-O or 2/1/1). The sericite 2M1 is part of the mica family and has a structure of type (T-O-T or 2/1). The non-clay phase is the quartz which disappears according to the efficient purification of the natural clays by the sedimentation method [16]. When ZnO loading, The XRD pattern of ZnO/CNA material indicates the existence of the ZnO zincite phase, and the appearance of diffraction peaks at 2θ is estimated to be 31.73, 34.44, 36.29, 47.52, 56.63, and 62.82° belongs to the hexagonal crystal lattices (100), (002), (101), (102), (110), and (103), respectively [14, 24]. The low-intensity peaks in ZnO/CNA material may be associated with deeper permeation of the ZnO in the sheets of the clay structure [12]. The results obtained are in accordance with previous works on clay supported by ZnO [25-27]. The calcination at 500

°C leads to notable appearance of crystallites of pure ZnO on the clay. Photocatalytic activity agrees well with a smaller size of ZnO particles in the matrix [28].

*Scanning electron microscopy analysis*

The images of CNA and ZnO/CNA materials are shown in Figure 3 which clarifies that the morphological features were changed significantly upon an impregnation process. The SEM micrograph of CNA showed that the surface clay is close-compact and layered structure and this is because of the elimination of impurities using the sedimentation method [29]. Obviously, the surface morphology of CNA (Figure 3**a**) is different from ZnO/CNA material (Figure 3**b**). It is clear from Figure 3**b** that the existence of ZnO facilitates adhering to the clay surface and exhibiting good dispersion [9, 30].

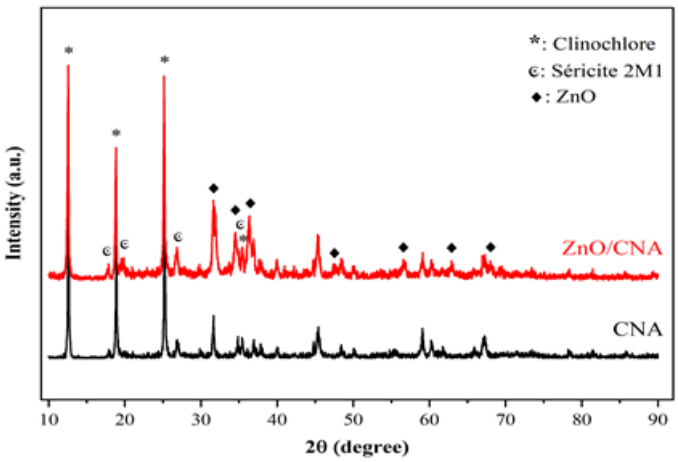


**Figure 2:** XRD patterns of CNA and ZnO/CAN

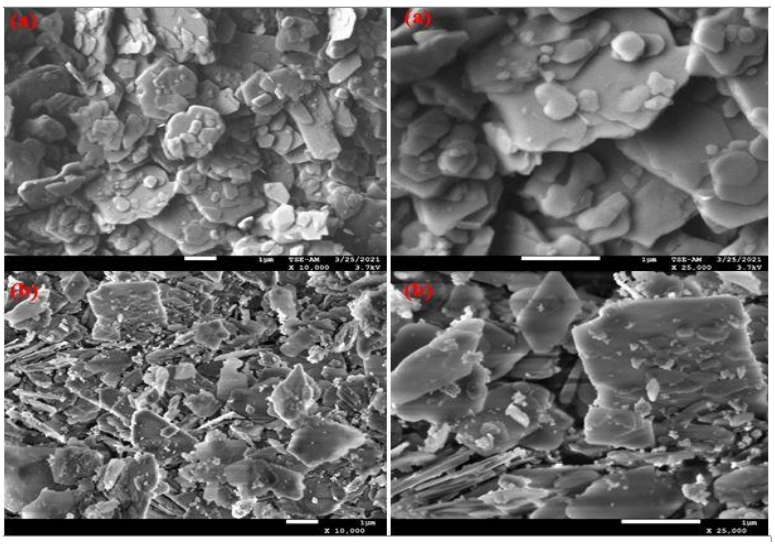

**Figure 3:** The SEM images of a) CNA and b) ZnO/CNA

*Energy dispersive X-ray spectroscopy analysis*

The EDS spectrum and ZnO/CNA elemental mapping images are presented in Figure 4. The EDS spectrum exhibits the existence of Zn on the material surface as well as clear peaks related to Al, Mg, O, Mn, and Si, which are considered the mineral composition of the CNA. The EDS elemental mapping images proved the existence of Zn and O in the ZnO/CNA material. The morphological studies of SEM and EDS with elemental mappings confirmed the successful formation of ZnO adhering to the surface clay [12].

*Adsorption studies*

*Adsorption kinetics studies*

The adsorption kinetic study of CV dye onto CNA or ZnO/CNA materials in aqueous solutions was implicated in determining the equilibrium time. Figure 5 represents the experiments data plots of adsorption capacity (qe) vs. time, which show that the amount of CV dye adsorbed increased rapidly for the two materials in the first 10 minutes and the CV removal efficiency was found to be 55% and 65% for CNA and ZnO/CNA, respectively. After 60 minutes, the adsorption capacity remains constant gradually up to the state of equilibrium which corresponds to the availability of the adsorption active sites on the material surface at the beginning of the process and it decreases progressively over time. The maximum adsorption amount of CV dye at equilibrium time equals 38.01 mg/g and 41.13 mg/g for CNA and ZnO/CNA, respectively. The results show that the equilibrium time was 60 minutes. The difference in capacity between the two materials is related to electrostatic attraction [31].

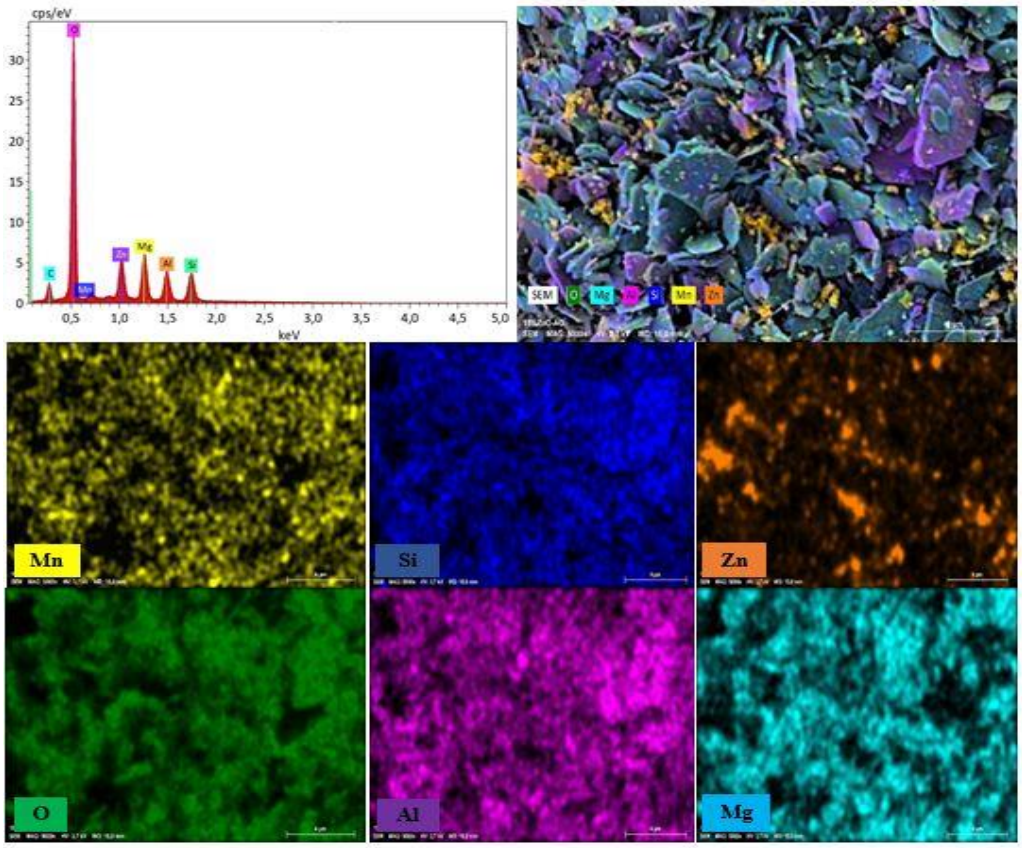


**Figure 4:** EDS spectrum and elemental mapping images for ZnO/CAN

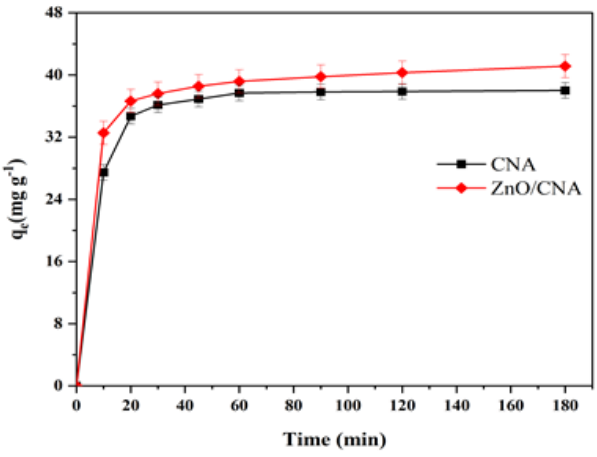


**Figure 5:** The effect of contact time in CV adsorption over CNA or ZnO/CNA; (catalyst dose = 0.5 g/L, concentration initial of CV = 25 mg/L, pH = 6.7 and room temperature

The adsorption process kinetics were studied with four models including pseudo-1st order, pseudo-second-order, Elovich, and intraparticle diffusion kinetic models to investigate the rate and mechanism of the adsorption process [17]; these kinetic models equations are respectively given by:

$$\ln(q_e - q_t) = lnq_e - k_1 t \quad (3)$$

$$\frac{t}{q_t} = \frac{1}{k_2\, q_e^2} + \frac{t}{q_e} \quad (4)$$

$$q_t = \frac{1}{\beta} + \frac{1}{\beta}\ln t \quad (5)$$

$$q_t = k_{int} t^{0.5} + C \quad (6)$$

where $q_e$ and $q_t$ (mg/g) are the dye amount adsorbed at time t and equilibrium, respectively, t is the time (min); $k_1$ ($min^{-1}$) and $k_2$ (g/mg min) are the pseudo-1st order and second-order models rate constants, respectively; α (mg/g min) and β (g/mg) are initial rate adsorption and the desorption rate, respectively; $k_{int}$ (mg/g $min^{0.5}$) and C (mg/g) are rates constant of intra-particle diffusion and constantly associated with the boundary layer thickness, respectively. The pseudo-1st order kinetic model values $k_1$ and $q_e$ are calculated from the plots *Ln ($q_e$-$q_t$) vs. t*, while the second-order kinetic model values $k_2$ and $q_e$ are determined by the linear fit of plots *$t/q_t$ vs. t*. The parameters of the adsorption kinetics with the correlation coefficients ($R^2$) are given in Table 2.

**Table 2:** The kinetics parameters of CV adsorption over CNA or ZnO/CNA

| Model | Parameters | | CNA | ZnO/CNA |
|---|---|---|---|---|
| Pseudo-1st order | $q_{e\text{-}exp}$ (mg/g) | | 38.01 | 41.13 |
| | $k_1$ ($min^{-1}$) | | 0.0738 | 0.044 |
| | $q_{1e}$ (mg/g) | | 23.58 | 18.52 |
| | $R^2$ | | 0.95 | 0.79 |
| Pseudo-second-order | $k_2$ (g/mg min) | | 0.0106 | 0.0071 |
| | $q_{2e}$ (mg/ g) | | 38.61 | 41.66 |
| | $R^2$ | | 0.99 | 0.99 |
| Elovich | β (g/mg) | | 0.224 | 0.315 |
| | α (mg/g min) | | 343.74 | 12396.85 |
| | $R^2$ | | 0.82 | 0.92 |
| Intra particle diffusion | $K_{id}$ (mg/g $min^{1/2}$) | $d_1$ | 7.9291 | 8.5826 |
| | | $d_2$ | 0.8742 | 0.7711 |
| | | $d_3$ | 0.0553 | 0.3448 |
| | C (mg/g) | $d_1$ | 0.5409 | 1.2242 |
| | | $d_2$ | 31.023 | 33.287 |
| | | $d_3$ | 37.266 | 36.511 |
| | $R^2$ | $d_1$ | 0.99 | 0.97 |
| | | $d_2$ | 0.96 | 0.99 |
| | | $d_3$ | 0.99 | 0.99 |

Figure 6**a-d** shows the kinetic models' linear plots. It is concluded from these results that the linear model of second-order (*Eq. 4*) is the best fit model to describe the experimental data of the adsorption kinetics of CV removal. The higher values of $R^2$ (> 0.99) for the second-order indicate a mechanism of chemisorption type adsorption, implying a valence force between adsorbate and adsorbent via sharing or exchanging electrons. The calculated values by second-order of the adsorbed amount ($q_{2e}$) at equilibrium and the experimental values ($q_{e\text{-}exp}$) are very close compared with other models, which denote the applicability of this model. The calculated values ($q_{1e}$) at equilibrium by the first-order kinetic (*Eq. 3*) are relatively small compared with the experimental quantity ($q_{e\text{-}exp}$) for the adsorption process. Similar results were found recently in the adsorption of CV onto smectite clay [17] and on montmorillonite nanocomposite intercalated by graphene oxide [31].

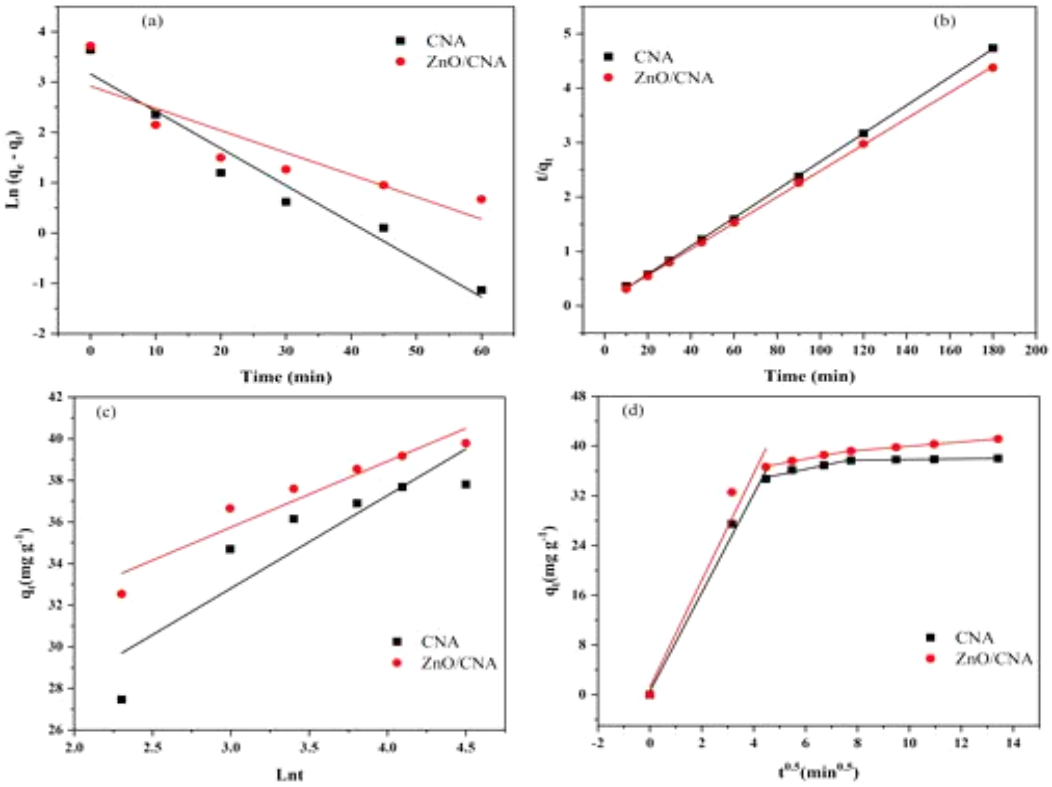


**Figure 6:** The kinetics models of CV adsorption over different materials: pseudo-1st order (a), pseudo-second-order (b), Elovich (c), and intraparticle diffusion (d); (catalyst dose = 0.5 g/L, concentration initial of CV = 25 mg/L, pH = 6.7 and room temperature)

The kinetic constants α and β of the Elovich model (*Eq. 5*) were calculated by the linear fit of plots *qt vs. lnt*, respectively. The higher values of α than β indicate that the adsorption rate was higher than that of desorption, which confirmed the viability of the adsorption process [32, 33].

The intraparticle diffusion model (*Eq. 6*) is widely applied to investigate the adsorption process mechanism. The kinetic constants values $k_{int}$ and C were determined from the plots *qt vs.* $t^{0.5}$, respectively, when the C values increase, the boundary layer effect also increases. The plots present three different regions for each material indicating three types of diffusion were influenced in the rate-limiting steps. The rate constants show that there is a gradual decrease in the adsorption over time. The initial portion $d_1$ represents the adsorption rapid of CV dye molecules via boundary layer diffusion, where CV dye molecules were positioned on the material external surface and tend to cover the material surface mesopores. The second portion $d_2$ is a gradual adsorption stage where the CV molecules are diffusing slowly and adsorbing into the material pores. The last portion $d_3$ relates to the adsorption equilibrium stage, where the diffusion process rate becomes very slow due to the decrease in the adsorbate concentration [24, 34].

*Effect of pH*

pH is considered one of the essential parameters of the adsorption process. Thus, it has an important influence on the adsorption capacity of the materials because it affects the adsorbent surface charge properties, the charge of the molecule, and the interaction between the organic molecules and the materials surface [17]. The pH varied from 2 to 11 in the initial CV solution (25 mg/L) with 0.025 g of materials (CNA or ZnO/CNA) at ambient temperature. The results in Figure 7 show in low pH value (pH < 4.2) the removal rate of CV is low, and this happens by the competition between the cations of CV dye and the $H^+$ protons for the active sites of materials [35]. When pH increases, the adsorption capacity increases as well, due to the highly negatively charged material surface, and the association between the material surface and the cationic dye

was more facilitated [36]. At high pH (pH > 8.2) the fixing rate decreased gradually for the reason of the occurrence of repulsive forces between the material surface strongly negatively charged and free CV dye electron pairs. We conclude that the removal of CV followed the mechanism of the electrostatic interactions [18]. Moreover, the maximum amount adsorbed of CV dye at equilibrium is observed at neutral medium pH (6.3 - 7.2) for the two materials. For this reason, a pH of 6.7 was chosen as the optimal value for the present study.

*Adsorption isotherms studies*

The study of adsorption isotherm was conducted to clarify the interaction between molecules of CV dye and the materials [37]. The adsorption equilibrium data were studied using the two most widely models, i.e. Freundlich and Langmuir.

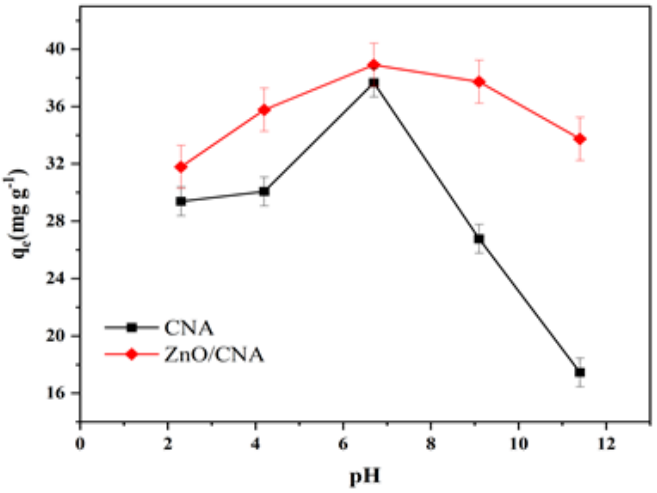


**Figure 7:** The pH effect in CV adsorption over CNA or ZnO/CNA

The adsorption isotherm experiments were investigated using 50 mL of CV solution with different initial dye concentrations (5 to 200 mg/L) at ambient temperature. The Freundlich and Langmuir isotherm model equations are expressed as:

$$q_e = K_f * C_e^{1/n} \quad (7)$$

$$\frac{Ce}{qe} = \frac{1}{K_L q_0} + \frac{1}{q_0} * C_e \quad (8)$$

where $q_e$ and $q_0$ (mg/g) are the adsorption quantity at equilibrium and the adsorption capacity maximum, respectively; $C_e$ (mg/L) is the concentration at equilibrium, $K_F$ (mg/g) (L/mg)$^{1/n}$ and n are Freundlich constants, and $K_L$ (L/mg) is constant of Langmuir. The isotherm parameters determined from the two models are presented in Table 3.

**Table 3:** The isotherm parameters of Langmuir and Freundlich models

| | Langmuir model | | | Freundlich model | | |
|---|---|---|---|---|---|---|
| Material | $q_0$ | $K_L$ | $R^2$ | $K_F$ | 1/n | $R^2$ |
| CNA | 72.46 | 0.104 | 0.99 | 14.689 | 0.332 | 0.98 |
| ZnO/CNA | 74.63 | 0.133 | 0.99 | 15.551 | 0.340 | 0.92 |

The correlation coefficients ($R^2$) from model plots (Figure 8) denoted that the best fits were obtained by the Langmuir model, considered as suited to adsorption isotherm data. They therefore signify the formation of homogeneous monolayer coverage of CV molecules on the material surface. This interaction is characterized by a homogeneous distribution of adsorptive sites, energetically equivalent, and without interaction between adsorbate molecules, which will lead to a linear isotherm [36]. The adsorption capacity according to the isotherm model of Langmuir equals 72.46 mg/g and 74.62 mg/g using CNA and ZnO/CNA materials, respectively. Also, the results

show that 1/n ranged from 0.33 to 0.34 indicating that the process is physisorption [38].

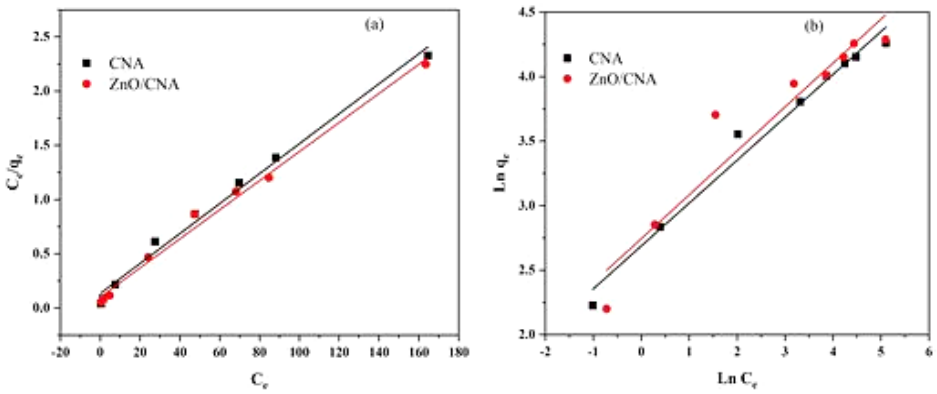


**Figure 8:** The isotherms models of CV adsorption over different materials: Langmuir (a) and Freundlich (b); (catalyst dose = 0.5 g/L, pH = 6.7 and room temperature)

*Thermodynamic studies*

The experiments' thermodynamics were examined using three temperatures 313 K, 323 K, and 333 K at pH 6.7. The essential parameters in the thermodynamic study are free energy change ($\Delta G°$), standard enthalpy ($\Delta H°$), and entropy change ($\Delta S°$) calculated by [31]:

$$K_d = q_e/C_e \quad (9)$$

$$\Delta G° = -RTlnK_d \quad (10)$$

$$lnK_d = \frac{\Delta S°}{R} - \frac{\Delta H°}{RT} \quad (11)$$

where R (8.314 J/mol K) denotes the constant of the ideal gas; T (K) is the absolute temperature; and $K_d$ (L/g) is the coefficient of sorption distribution. The $\Delta H°$ and $\Delta S°$ values are obtained by the linear fit of plots $LnK_d$ *vs.* $T^{-1}$ (Figure 9) and the results of thermodynamic parameters are illustrated in Table 4.

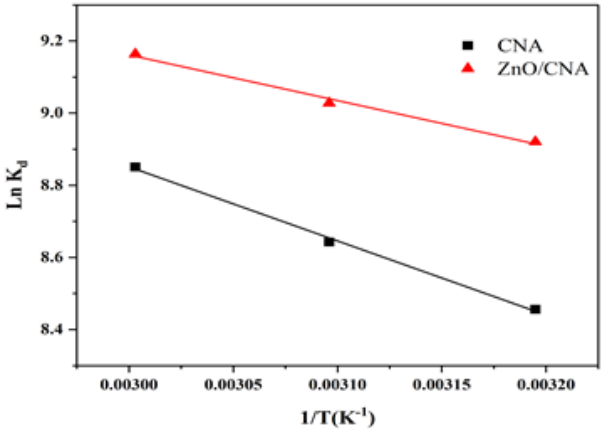


**Figure 9:** The temperature effect in CV adsorption over CNA or ZnO/CN

**Table 4:** The thermodynamic parameters of CV adsorption over CNA or ZnO/CNA

| Material | T(K) | $R^2$ | ΔH° (kJ/mol) | ΔS° (kJ/mol K) | ΔG° (kJ/mol) |
|---|---|---|---|---|---|
| CNA | 313<br>323<br>333 | 0.99 | 17.078 | 0.125 | -22.01<br>-23.21<br>-24.50 |
| ZnO/CNA | 313<br>323<br>333 | 0.99 | 10.515 | 0.108 | -23.21<br>-24.24<br>-25.36 |

The $\Delta G°$ values are negative for all the materials in the temperatures range (313 to 333 K). The negative $\Delta G°$ values signify that the adsorption process is spontaneous and physisorption because the $\Delta G°$ values are close to the physisorption range (0 to -20 kJ/mol) and lower than that of chemisorption (-80 to -400 kJ/mol) [39]. The ΔG° values get more negative when the temperature increases, indicating the increase in the adsorption capacity. The positive values of $\Delta H°$ are also in the physisorption range (1 to 93 kJ/mol) denoting that the process is endothermic [3]. The good affinity between the molecules of CV dye and the materials is demonstrated by the positive ΔS° values. The thermodynamic data coincides with works of literature [40].

*Adsorption/photocatalytic degradation studies*

The experimental results of the simultaneous effect of adsorption/photocatalytic degradation in the discoloration of CV using CNA or ZnO/CNA materials as presented in Figure 10**a**. The pure photolysis results of CV give a negligible degradation using UV-solar in the absence of any material during 120 min. The removal of CV gives about 35.2% and 41.8% using CNA and ZnO/CNA materials, respectively, during 60 min in the dark at room temperature, which is attributed to the CV molecules' adsorption [41]. We added zinc oxide as an active phase which has a positive effect through performing as a promoter of the photocatalytic activity. This addition has efficient effects on the adsorption and photo-degradation performance [42, 43]. Under sunlight, the activated CV molecules were converted to species of free transient radicals active of short duration in contact with the surfaces of ZnO transferring the negative charge produced [11]. The ZnO/CNA material gives better reactivity with a degradation reaching 49.7% compared with the CNA giving a degradation rate of 31.8% for sunlight irradiation time of 120 min. The Eg values of ZnO/CNA are between 2.98 and 3.10 eV, representing values characteristic valuable potentially for the photocatalytic experiments [25]. Particularly, the ZnO/CNA material showed the highest efficiency (Figure 10a) almost 92% discoloration of CV at 180 min during both adsorption and photodegradation experiments, whereas only 67% of CV was discolored using CNA alone. The discoloration of CV is enhanced by ZnO/CNA material depending on the synergistic effect of adsorption and photodegradation [18].

The photocatalytic degradation kinetic of CV using CNA or ZnO/CNA materials is illustrated by the pseudo-1st order model [44], and can be expressed by the equation below:

$$ln\frac{C_0}{C} = k_{app}t \qquad (12)$$

where $C_0$ (mg/L) and C (mg/L) are concentrations dye initially at solar irradiation time (t = 0) and at time t, respectively; $k_{app}$ ($min^{-1}$) is the apparent 1st order rate constant; and t (min) is the irradiation time. The linear plots *ln (C₀/C) vs. t* for the photodegradation kinetics of CV are shown in Figure 10b.

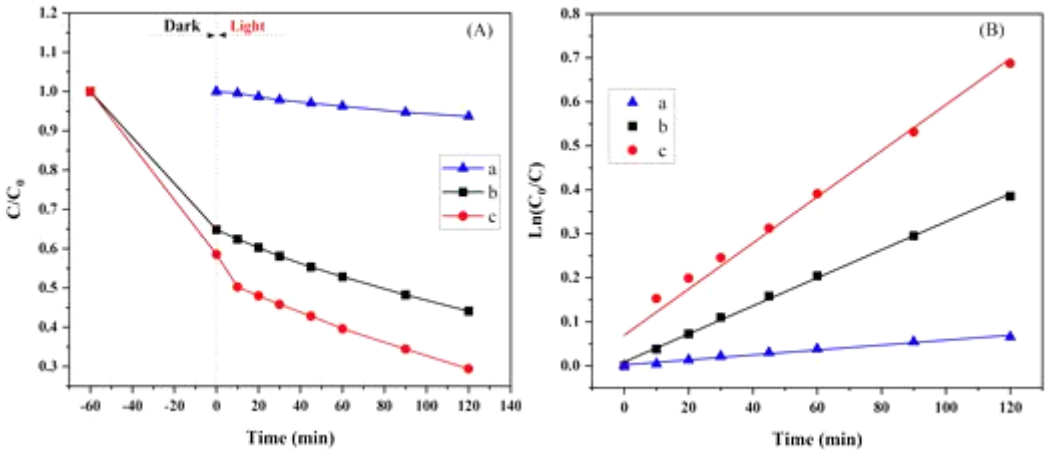


**Figure 10:** Adsorption/photocatalytic degradation of CV (A) and pseudo-1st order kinetic of CV degradation (B) at different conditions: (a) UV-Solar only, (b) UV-Solar/CNA, (c) UV-Solar/ZnO- CNA; (catalyst dose = 0.5 g/L, concentration initial of CV = 50 mg/L, pH = 6.7 and room temperature)

The plots (Figure 10b) showed good linear correlations denoting that the degradation kinetics of CV dye solution by CNA or ZnO/CNA materials were followed by the pseudo-1st order kinetic model. The correlation coefficients ($R^2$) from the plots are 0.99 and 0.98 for CNA and ZnO/CNA materials, respectively, corresponding to apparent rate constants $k_{app}$ by 0.0032 and 0.0052 $min^{-1}$. Thus, the ZnO/CNA material presented good activity in the photodegradation of CV under direct sunlight.

## Conclusion

The ZnO-supported natural volcanic Algerian clay (ZnO/CNA) was successfully used as a highly efficient adsorbent and photocatalyst. The discoloration of CV from an aqueous solution followed two mechanisms, i.e. adsorption and photo-degradation. The XRD patterns of materials revealed the existence of three phases, Clinochlore, Sericite 2M1, and the ZnO zincite phase as evidenced by EDX and SEM analyses. The experimental results show that the pseudo-second and pseudo-1st order models described the adsorption and degradation kinetics, respectively. Isotherm studies fit best with the Langmuir model. The adsorption capacities maximum calculated by the Langmuir equation is 72.46 and 74.62 mg/g for CNA and ZnO/CNA materials, respectively. Moreover, thermodynamic studies revealed that the CV dye solution adsorption on these samples was found to be spontaneous, physisorption, and endothermic. The photo-degradation experiments indicated that the ZnO/CNA material was presenting the best performance for the discoloration of CV dye solution in solar irradiation. From this work, we found that the synergetic effect of adsorption/photodegradation is promising and examined in the discoloration of CV dye solution.

## Acknowledgments

The authors are deeply grateful to the Algerian Ministry of Higher Education and Scientific Research.

## Ethical issue

Authors are aware of and comply with, best practices in publication ethics specifically authorship (avoidance of guest authorship), dual submission, manipulation of figures, competing interests, and compliance with policies on research ethics. Authors adhere to publication requirements that the submitted work is original and has not been published elsewhere in any language.

## Competing interests

The authors declare that no conflict of interest would prejudice the impartiality of this scientific work.

## Authors' contribution

All authors of this study have a complete contribution to data collection, data analyses, and manuscript writing.

**ORCID:**

*Zakarya Ayoub Messaoudi*
https://orcid.org/0000-0003-0532-2722
*Driss Lahcene*
https://www.orcid.org/0000-0001-8701-906X
*Mohammed Messaoudi*
https://www.orcid.org/0000-0001-9893-5987
*Meriem Belhachemi*
https://www.orcid.org/0000-0002-6014-4765
*Abderrahim Choukchou-Braham*
https://www.orcid.org/0000-0003-1491-1924

## References

[1]. Konicki W., Aleksandrzak M., Mijowska E., Equilibrium, kinetic and thermodynamic studies on adsorption of cationic dyes from aqueous solutions using graphene oxide, *Chemical Engineering Research and Design*, 2017, **123**:35 [Crossref], [Google Scholar], [Publisher]

[2]. Youcef L.D., Belaroui L.S., López-Galindo A., Adsorption of a cationic methylene blue dye on an Algerian palygorskite, *Applied Clay Science*, 2019, **179**:105145 [Crossref], [Google Scholar], [Publisher]

[3]. Omer O.S., Hussein M.A., Hussein B.H.M., Mgaidi A., Adsorption thermodynamics of cationic dyes (methylene blue and crystal violet) to a natural clay mineral from aqueous solution between 293.15 and 323.15 K, *Arabian Journal of Chemistry*, 2018, **11**:615 [Crossref], [Google Scholar], [Publisher]

[4]. Sarabadan M., Bashiri H., Mousavi S.M., Adsorption of crystal violet dye by a zeolite-montmorillonite nano-adsorbent: modelling, kinetic and equilibrium studies, *Clay Minerals*, 2019, **54**:357 [Crossref], [Google Scholar], [Publisher]

[5]. Brião G.V., Jahn S.L., Foletto E.L., Dotto G.L., Adsorption of crystal violet dye onto a mesoporous ZSM-5 zeolite synthetized using chitin as template, *Journal of Colloid and Interface Science*, 2017, **508**:313 [Crossref], [Google Scholar], [Publisher]

[6]. Jayasantha Kumari H., Krishnamoorthy P., Arumugam T.K., Radhakrishnan S., Vasudevan D., An efficient removal of crystal violet dye from waste water by adsorption onto TLAC/Chitosan composite: A novel low cost adsorbent, *International Journal of Biological Macromolecules*, 2017, **96**:324 [Crossref], [Google Scholar], [Publisher]

[7]. Sarabadan M., Bashiri H., Mousavi S.M., Removal of crystal violet dye by an efficient and low cost adsorbent: Modeling, kinetic, equilibrium and thermodynamic studies, *Korean Journal of Chemical Engineering*, 2019, **36**:1575 [Crossref], [Google Scholar], [Publisher]

[8]. Esmaeili H., Hashemi S.A.A., Clay/MgFe2O4 as a Novel Composite for Removal of Cr (VI) From Aqueous Media, *ChemistrySelect*, 2020, **5**:9377 [Crossref], [Google Scholar], [Publisher]

[9]. Zyoud A.H., Asaad S., Zyoud S.H., Zyoud S.H., Helal M.H., Qamhieh N., Hajamohideen A.R., Hilal H.S., Raw clay supported ZnO nanoparticles in photodegradation of 2-chlorophenol under direct solar radiations, *Journal of Environmental Chemical Engineering*, 2020, **8**:104227 [Crossref], [Google Scholar], [Publisher]

[10]. Hassanimarand M., Anbia M., Salehi S., Removal of Acid Blue 92 by Using Amino-Functionalized Silica-Pillared Clay as a New Nano-Adsorbent: Equilibrium, *Kinetic and Thermodynamic Parameters*, 2020, **5**:6141 [Crossref], [Google Scholar], [Publisher]

[11]. Mohanty S., Moulick S., Maji S.K., Adsorption/photodegradation of crystal violet (basic dye) from aqueous solution by hydrothermally synthesized titanate nanotube (TNT), *Journal of Water Process Engineering*, 2020, **37**:101428 [Crossref], [Google Scholar], [Publisher]

[12]. Misra A.J., Das S., Rahman A.P.H., Das B., Jayabalan R., Behera S.K., Suar M., Tamhankar A.J., Mishra A., Lundborg C.S., Tripathy S.K., Doped ZnO nanoparticles impregnated on Kaolinite (Clay): A reusable nanocomposite for photocatalytic disinfection of multidrug resistant Enterobacter sp. under visible light, *Journal of Colloid and Interface Science*, 2018, **530**:610 [Crossref], [Google Scholar], [Publisher]

[13]. Zyoud A.H., Zubi A., Zyoud S.H., Hilal M.H., Zyoud S., Qamhieh N., Hajamohideen A., Hilal H.S., Kaolin-supported ZnO nanoparticle catalysts in self-sensitized tetracycline photodegradation: Zero-point charge and pH effects, *Applied Clay Science*, 2019, **182**:105294 [Crossref], [Google Scholar], [Publisher]

[14]. Hadjltaief H.B., Ameur S.B., Da Costa P., Ben Zina M., Elena Galvez M. Photocatalytic decolorization of cationic and anionic dyes over ZnO nanoparticle immobilized on natural Tunisian clay, *Applied Clay Science*, 2018, **152**:148 [Crossref], [Google Scholar], [Publisher]

[15]. Hadjltaief H.B., Gálvez M.E., Zina M.B., Da Costa, P., Da Costa P. TiO2/clay as a heterogeneous catalyst in photocatalytic/photochemical oxidation of anionic reactive blue 19, *Arabian Journal of Chemistry*, 2019, **12**:1454 [Crossref], [Google Scholar], [Publisher]

[16]. Lahcene D., Behilil A., Zahraoui B., Benmehdi H., Belhachemi M., Choukchou-Braham A., Physicochemical characterization of new natural clay from south west of Algeria: Application to the elimination of malachite green dye, *Environmental Progress & Sustainable Energy*, 2019, **38**:13152 [Crossref], [Google Scholar], [Publisher]

[17]. Hamza W., Dammak N., Hadjltaief H.B., Eloussaief M., Benzina M., Sono-assisted adsorption of Cristal Violet dye onto Tunisian Smectite Clay: Characterization, kinetics and adsorption isotherms, *Ecotoxicology and Environmental Safety*, 2018, **163**:365 [Crossref], [Google Scholar], [Publisher]

[18]. Ullah R., Sun J., Gul A., Bai S., One-step hydrothermal synthesis of TiO2-supported clinoptilolite: An integrated photocatalytic adsorbent for removal of crystal violet dye from aqueous media, *Journal of Environmental Chemical Engineering*, 2020, **8**:103852 [Crossref], [Google Scholar], [Publisher]

[19]. Marushchenko L.I., Baksheev I.A., Nagornaya E.V., Chitalin A.F., Nikolaev Y.N., Kal'ko

I.A., Prokofiev V.Y., Quartz-sericite and argillic alterations at the Peschanka Cu-Mo-Au deposit, Chukchi Peninsula, Russia, *Geology of Ore Deposits*, 2015, **57**:213 [Crossref], [Google Scholar], [Publisher]

[20]. Moro D., Ulian G., Valdrè G., 3D meso-nanostructures in cleaved and nanolithographed Mg-Al-hydroxysilicate (clinochlore): Topology, crystal-chemistry, and surface properties, *Applied Clay Science*, 2019, **169**:74 [Crossref], [Google Scholar], [Publisher]

[21]. Miranda M.O., Viana B.C., Honório L.M., Trigueiro P., Fonseca M.G., Franco F., Osajima J.A., Silva-Filho E.C., Oxide-Clay Mineral as Photoactive Material for Dye Discoloration, *Minerals*, 2020, **10**:132 [Crossref], [Google Scholar], [Publisher]

[22]. Choi H.J., Application of methyl-esterified sericite for harvesting microalgae species, *Journal of Environmental Chemical Engineering*, 2016, **4**:3593 [Crossref], [Google Scholar], [Publisher]

[23]. Gupta G.S., Senapati V.A., Dhawan A., Shanker R., Heteroagglomeration of zinc oxide nanoparticles with clay mineral modulates the bioavailability and toxicity of nanoparticle in Tetrahymena pyriformis, *Journal of Colloid and Interface Science*, 2017, **495**:9 [Crossref], [Google Scholar], [Publisher]

[24]. Mohamed S.K., Hegazy S.H., Abdelwahab N.A., Ramadan A.M., Coupled adsorption-photocatalytic degradation of crystal violet under sunlight using chemically synthesized grafted sodium alginate/ZnO/graphene oxide composite, *International Journal of Biological Macromolecules*, 2018, **108**:1185 [Crossref], [Google Scholar], [Publisher]

[25]. Akkari M., Aranda P., Ben Rhaiem H., Ben Haj Amara A., Ruiz-Hitzky E., ZnO/clay nanoarchitectures: Synthesis, characterization and evaluation as photocatalysts, *Applied Clay Science*, 2016, **131**:131 [Crossref], [Google Scholar], [Publisher]

[26]. Sani H.A., Ahmad M.B., Hussein M.Z., Ibrahim N.A., Musa A., Saleh T.A., Nanocomposite of ZnO with montmorillonite for removal of lead and copper ions from aqueous solutions, *Process Safety and Environmental Protection*, 2017, **109**:97 [Crossref], [Google Scholar], [Publisher]

[27]. Ye J., Li X., Hong J., Chen J., Fan Q., Photocatalytic degradation of phenol over ZnO nanosheets immobilized on montmorillonite, *Materials Science in Semiconductor Processing*, 2015, **39**:17 [Crossref], [Google Scholar], [Publisher]

[28]. Janíková B., Tokarský J., Mamulová Kutláková K., Kormunda M., Neuwirthová L., Photoactive and non-hazardous kaolin/ZnO composites prepared by calcination of sodium zinc carbonate, *Applied Clay Science*, 2017, **143**:345 [Crossref], [Google Scholar], [Publisher]

[29]. Dhakshinamoorthy A., Visuvamithiran P., Tharmaraj V., Pitchumani K., Clay encapsulated ZnO nanoparticles as efficient catalysts for N-benzylation of amines, *Catalysis Communications*, 2011, **16**:15 [Crossref], [Google Scholar], [Publisher]

[30]. Abdullah N.H., Shameli K., Abdullah E.C., Abdullah L.C., Low cost and efficient synthesis of magnetic iron oxide/activated sericite nanocomposites for rapid removal of methylene blue and crystal violet dyes, *Materials Characterization*, 2020, **163**:110275 [Crossref], [Google Scholar], [Publisher]

[31]. Puri C., Sumana G., Highly effective adsorption of crystal violet dye from contaminated water using graphene oxide intercalated montmorillonite nanocomposite, *Applied Clay Science*, 2018, **166**:102 [Crossref], [Google Scholar], [Publisher]

[32]. Ahamad K.U., Singh R., Baruah I., Choudhury H., Sharma M.R., Equilibrium and kinetics modeling of fluoride adsorption onto activated alumina, alum and brick powder, *Groundwater for Sustainable Development*, 2018, **7**:452 [Crossref], [Google Scholar], [Publisher]

[33]. 33. Sevim F, Lacin O, Ediz EF, Demir F. Adsorption capacity, isotherm, kinetic, and thermodynamic studies on adsorption behavior of malachite green onto natural red clay, *Environmental Progress & Sustainable Energy*, 2021, **40**:e13471 [Crossref], [Google Scholar], [Publisher]

[34]. Belhachemi M., Djelaila S., Removal of Amoxicillin Antibiotic from Aqueous Solutions by Date Pits Activated Carbons, *Environmental Processes*, 2017, **4**:549 [Crossref], [Google Scholar], [Publisher]

[35]. Liu X., Liu Y., Lu S., Guo W., Xi B., Performance and mechanism into TiO2/Zeolite composites for sulfadiazine adsorption and photodegradation, *Chemical Engineering Journal*, 2018, **350**:131 [Crossref], [Google Scholar], [Publisher]

[36]. Ngoc Hoang B., Thi Nguyen T., Van Nguyen D., Van Tan L., Removal of crystal violet from aqueous solution using environment-friendly and water-resistance membrane based on polyvinyl/agar/maltodextrin, *Materials Today: Proceedings*, 2021, **38**:3046 [Crossref], [Google Scholar], [Publisher]

[37]. Fabryanty R., Valencia C., Soetaredjo F.E., Putro J.N., Santoso S.P., Kurniawan A., Ju Y.H., Ismadji S., Removal of crystal violet dye by adsorption using bentonite – alginate composite, *Journal of Environmental Chemical Engineering*, 2017, **5**:5677 [Crossref], [Google Scholar], [Publisher]

[38]. Liu S., Liu Y., Jiang L., Zeng G., Li Y., Zeng Z., Wang X., Ning Q., Removal of 17β-Estradiol from water by adsorption onto montmorillonite-carbon hybrids derived from pyrolysis carbonization of carboxymethyl cellulose, *Journal of Environmental Management,* 2019, **236**:25 [Crossref], [Google Scholar], [Publisher]

[39]. Sharma P., Borah D.J., Das P., Das M.R., Cationic and anionic dye removal from aqueous solution using montmorillonite clay: evaluation of adsorption parameters and mechanism, *Desalination and Water Treatment*, 2016, **57**:8372 [Crossref], [Google Scholar], [Publisher]

[40]. Loulidi I., Boukhlifi F., Ouchabi M., Amar A., Jabri M., Kali A., Chraibi S., Hadey C., Aziz F., Adsorption of Crystal Violet onto an Agricultural Waste Residue: Kinetics, Isotherm, Thermodynamics, and Mechanism of Adsorption, *The Scientific World Journal*, 2020, **2020**:5873521. [Crossref], [Google Scholar], [Publisher]

[41]. Tobajas M., Belver C., Rodriguez J.J., Degradation of emerging pollutants in water under solar irradiation using novel TiO2-ZnO/clay nanoarchitectures, *Chemical Engineering Journal*, 2017, **309**:596 [Crossref], [Google Scholar], [Publisher]

[42]. Yusuff A.S., Taofeek Popoola L., Aderibigbe E.I., Solar photocatalytic degradation of organic pollutants in textile industry wastewater by ZnO/pumice composite photocatalyst, *Journal of Environmental Chemical Engineering*, 2020, **8**:103907 [Crossref], [Google Scholar], [Publisher]

[43]. Zyoud A.H., Zorba T., Helal M., Zyoud S., Qamhiya N., Hajamohideen A.R., Zyoud Sh., Hilal H.S., Direct sunlight-driven degradation of 2-chlorophenol catalyzed by kaolinite-supported ZnO, *International Journal of Environmental Science and Technology*, 2019, **16**:6267 [Crossref], [Google Scholar], [Publisher]

[44]. Hadjltaief H.B., Zina M.B., Galvez M.E., Da Costa P. Photocatalytic degradation of methyl green dye in aqueous solution over natural clay-supported ZnO–TiO2 catalysts, *Journal of Photochemistry and Photobiology A: Chemistry*, 2016, **315**:25 [Crossref], [Google Scholar], [Publisher]

**HOW TO CITE THIS ARTICLE**

Zakarya Ayoub Messaoudi, Driss Lahcene, Tahar Benaissa, Mohammed Messaoudi, Brahim Zahraoui Meriem Belhachemi, Abderrahim Choukchou-Braham, Adsorption and Photocatalytic Degradation of Crystal Violet Dye under Sunlight Irradiation Using Natural and Modified Clays by Zinc Oxide. *Chem. Methodol.*, 2022, 6(9) 661-676
https://doi.org/10.22034/CHEMM.2022.340376.1507
URL: http://www.chemmethod.com/article_152726.html